Journal of Pharmacological Sciences 131 (2016) 77–83

Contents lists available at ScienceDirect

Journal of Pharmacological Sciences

journal homepage: www.elsevier.com/locate/jphs

Full paper

Trichosanthin-induced autophagy in gastric cancer cell MKN-45 is dependent on reactive oxygen species (ROS) and NF-κB/p53 pathway

Bin Wei, Qiaoying Huang, Shunrong Huang, Wei Mai, Xiaogang Zhong*

People's Hospital of Guangxi Zhuang Autonomous Region, Nanning, 530000, Guangxi, China

ARTICLE INFO

Article history:
Received 28 January 2016
Received in revised form
29 February 2016
Accepted 1 March 2016
Available online 10 March 2016

Keywords:
Trichosanthin
Autophagy
Apoptosis
Gastric cancer
Reactive oxygen species

ABSTRACT

Trichosanthin (TCS), isolated from the root tuber of *Trichosanthes kirilowii* tubers in the Cucurbitaceae family, owns a great deal of biological and pharmacological activities including anti-virus and anti-tumor. TCS has been reported to induce cell apoptosis of a diversity of cancers, including cervical cancer, choriocarcinoma, and gastric cancer, etc. However, whether TCS would induce autophagy in gastric cancer cells was seldom investigated. In current study, human gastric cancer MKN-45 cell growth was significantly inhibited by TCS. The anti-proliferation effect of TCS was due to an increased autophagy, which was confirmed by monodansylcadervarine (MDC) staining, up-regulation of Autophagy protein 5 (Atg5), and conversion of LC3 I to LC3 II (autophagosome marker). In addition, TCS induced reactive oxygen species (ROS) in MKN-45 cells and ROS scavenger N-acetylcysteine (NAC) significantly reversed TCS-induced autophagy. Furthermore, NF-κB/p53 pathway was activated during the process of autophagy induced by TCS and the ROS generation was mediated by it in MKN-45 cells. *In vivo* results showed that TCS exerted significantly anti-tumor effect on MKN-45 bearing mice. Considering the clinical usage of TCS on other human diseases, these research progresses provided a new insight into cancer research and new therapeutic avenues for patients with gastric cancer.

1. Introduction

The catabolic process by which cells degrade their own constituents through the lysosomal pathway was known as autophagy. Autophagy maintains intracellular metabolic homeostasis through digesting some parts of intracellular materials (1). The multi-step process of autophagy is regulated by a large group of autophagy-related proteins (Atg), which were involved in the formation of autophagosomes (2). Another autophagosome related protein is microtubule-associated protein 1 light chain 3 (LC3). LC3 has two forms, LC3 I and LC3 II (3). LC3 II is present both inside and outside of autophagosomes, LC3 is widely used to monitor autophagy now. Various factors and signaling pathways are involved in autophagy. Among them, reactive oxygen species (ROS) are presented to be important signals activating autophagy.

Reactive oxygen species (ROS), which are integral components of multiple cellular pathways, plays an essential role in apoptosis and autophagy. ROS are generated from the mitochondria as well as other sources. It's reported that when antioxidant mechanisms are overwhelmed by ROS, cell damage and cell death occurs (4). There is an accumulation of evidence that highlights the relationship between the generation of ROS and cell death, including apoptosis and autophagy (5–7).

Nuclear factor kappa B (NF-κB), a protein of transcription factors, plays a key role in inflammation, immunity, proliferation as well as in cell death (8). Recent research proved that inhibition of autophagy will rescue NF-κB activity (9). It is well established that the activation of NF-κB is required for autophagy (10). Another research reported that upregulating the expression of NF-κB would induce autophagy (11). The tumor-suppressing transcription factor p53 is actively in response to a large number of cellular stresses signals, including carbon and oxygen deficiencies, genotoxic stress, and proliferation (12). Since p53 deeply involves in genotoxic stress response and DNA damage repair, it is capable of regulating autophagy (1,13,14).

Trichosanthin (TCS) is isolated from the root tuber of *Trichosanthes kirilowii* Maxim which has been traditionally used in China

* Corresponding author. Department of Gastroenterology and Peripheral Vascular Surgery, People's Hospital of Guangxi Zhuang Autonomous Region, No.66, Yaotao Road, Nanning, 530000, Guangxi, China.
E-mail address: xiaogaong_zhong88@126.com (X. Zhong).
Peer review under responsibility of Japanese Pharmacological Society.

http://dx.doi.org/10.1016/j.jphs.2016.03.001

as an abortifacient drug in early and midterm abortion (15). TCS is well known for its various pharmacological and physiological effects such as induction of abortion, anti-HIV and anti-HIV enzyme, neurotoxicity, inhibition of protein synthesis, anti-tumor and so on (16–20). In recent studies, TCS possessed anti-tumor activity in many tumor types including gastric tumor cells (20–24). However, the mechanisms of TCS-induced gastric cancer cells death were barely reported. The purpose of this study is to investigate the underlying action of TCS in MKN-45 human gastric cancer.

2. Materials and methods

2.1. Reagents

Trichosanthin with a purity of 98% was obtained from Sigma (St. Louis, MO, USA). TCS was dissolved in dimethylsulfoxide (DMSO) to make a stock solution. Then the stock solution was diluted with RPMI-1640 complete medium and the final concentration of DMSO was kept below 0.05% in cell culture to avoid detectable effects on cell growth and viability. Methylthiazolydiphenyl-tetrazoliumbromide (MTT), propidium iodide (PI), MDC, NAC, 3-MA were also bought from Sigma. Primary antibody against Atg5, LC3, phospho-NF-kB, phospho-p53 and secondary antibodies were acquired from Cell Signaling Technology (Danvers, MA, USA). NF-κB inhibitor CID2858522 and p53 inhibitor Pifithrin-β were purchased from SelleckChem (Radnor, PA, USA).

2.2. Cells and culture

Gastric cancer cell MKN-45 cells obtained from American Type Culture Collection (ATCC, Manassas, VA, USA) were cultured in RPMI-1640 medium (Invitrogen, Carlsbad, CA, USA) supplemented with 10% fetal bovine serum (FBS, Hyclone, Logan, UT, USA), streptomycin (100 U/mL) and penicillin (100 μg/mL) at 37 °C in a humidified atmosphere containing 5% CO_2. The cells were starved in medium supplemented with 1% FBS for 24 h before treatments.

2.3. Cytotoxicity assay

MKN-45 cells were plated at a density of 1×10^4 cells/well in 96-well cell culture plates (Corning, NY, USA) and cultured for 24 h. Then the cells were treated with indicated concentrations of TCS. After additional 24, 48 or 72 h incubation at 37 °C and 5% CO_2, the cells were rinsed twice with ice-cold PBS and then incubated with 100 μL of 0.5 mg/mL MTT solution for 3 h. The resulting crystal was dissolved in 150 μL DMSO and the optical density was measured by MTT assay using a micro-plate reader. Cell growth inhibitory ratio was calculated as followed:

$$\text{Cell growth inhibitory ratio (\%)} = 100 \times \left(A_{490,\text{control}} - A_{490,\text{sample}}\right) \Big/ \left(A_{490,\text{control}} - A_{490,\text{blank}}\right)$$

2.4. Cell apoptosis assays

Cell apoptosis was detected by Annexin V-FITC/PI Apoptosis Detection Kit (Pierce Biotechnology, Rockford, IL, USA). MKN-45 were cultured in 6-well plates (5×10^5/well) and treated with different concentrations of TCS. Then, the cells were washed with PBS and then collected. After labeled by annexin V-FITC and PI, the cells were analyzed using a flow cytometer.

2.5. Detection of caspase-3 activity

Cells (2×10^5) treated with different concentrations of TCS for indicated periods were collected and incubated for 10 min with chilled lysis buffer on ice, followed by centrifuged at 12,000 *g* for 3 min. The p-nitroanilide-conjugated substrate was added into the supernatants.

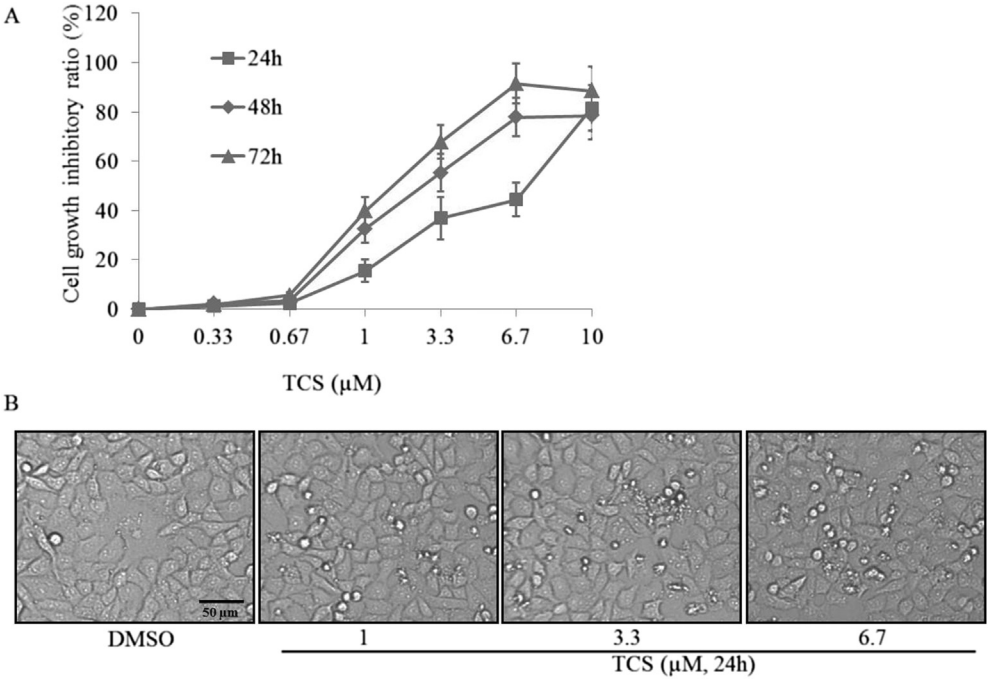

Fig. 1. Treatment with TCS induced the death of MKN-45 cells. (A) After the indicated dosage of TCS treatment for 24, 48 or 72 h, cell viability was assessed using the MTT assay at the sequential time points. Results are expressed as mean value ± SD, n = 3. (B) Morphologic changes of MKN-45 cells death were observed at 24 h (200× magnification).

After 1 h of incubation at 37 °C, detection of caspase-3 activity was performed at 405 nm. Protease units were quantified by comparison with a p-nitroanilide calibration curve, the value as followed:

Units of caspase-3 = (△A/h) × (1/slope of curve)

2.6. Western blotting analysis

The MKN-45 cells or tumors tissues were homogenized and lysed in cell lysis buffer (Bio-Rad Laboratories, Hercules, CA, USA) containing phosphatase inhibitor cocktail and proteinase inhibitor cocktail (Sigma), and the protein concentrations were determined using the BCA Protein Assay Kit (Pierce Biotechnology). 50 μg protein lysates were run on Bis-Tris gels (Thermo Fisher Scientific, Waltham, MA, USA) using MOPS buffer (Thermo Fisher). Proteins were transferred to nitrocellulose membranes by wet transfer or by iBlot (Invitrogen) dry transfer. Membranes were blocked in 5% skim-milk in 1 × PBS containing 0.01% Tween 20 (PBST) and were incubated with first or second antibodies in 5% skim-milk or 3% BSA in 1 × PBST, according to manufacturer's instructions. Membranes were washed with 1 × PBST and visualized with enhanced chemiluminescence (Amersham, GE Healthcare, Little Chalfont, UK). Relative proteins levels were quantified with Image Lab 4.1software (Bio-Rad).

2.7. In vivo xenograft tumor model

The MKN-45 cells were suspended in 100 μL RPMI-1640 medium adding another 100 μL Matrigel™ Matrix (BD, Biosciences Discovery Labware). Xenograft tumor model were established by implanting cells subcutaneously into female BALB/c nude mice (7 weeks old, 20–25 g), which were purchased from Shanghai SLAC Laboratory Animal Co., Ltd. (Shanghai, China). Mice were randomly assigned into four groups after two weeks tumor inoculation. The control group received saline once daily by oral administration for 3 weeks. The other three groups received different doses of TCS for 3 weeks (once daily, oral). The weights of the mice were monitor twice weekly. The mice were sacrificed and tumors were harvested in the end of efficacy study. All animal experiments were performed in accordance with protocols approved by the People's Hospital of Guangxi Experimental Animal Care and Use Committee.

2.8. Statistical analysis

All statistical analysis was performed with GraphPad Prism 4 software (Version 4.03, GraphPad Software, Inc., San Diego, CA, USA). Data was analyzed by ANOVA followed by Dunnett's test. All

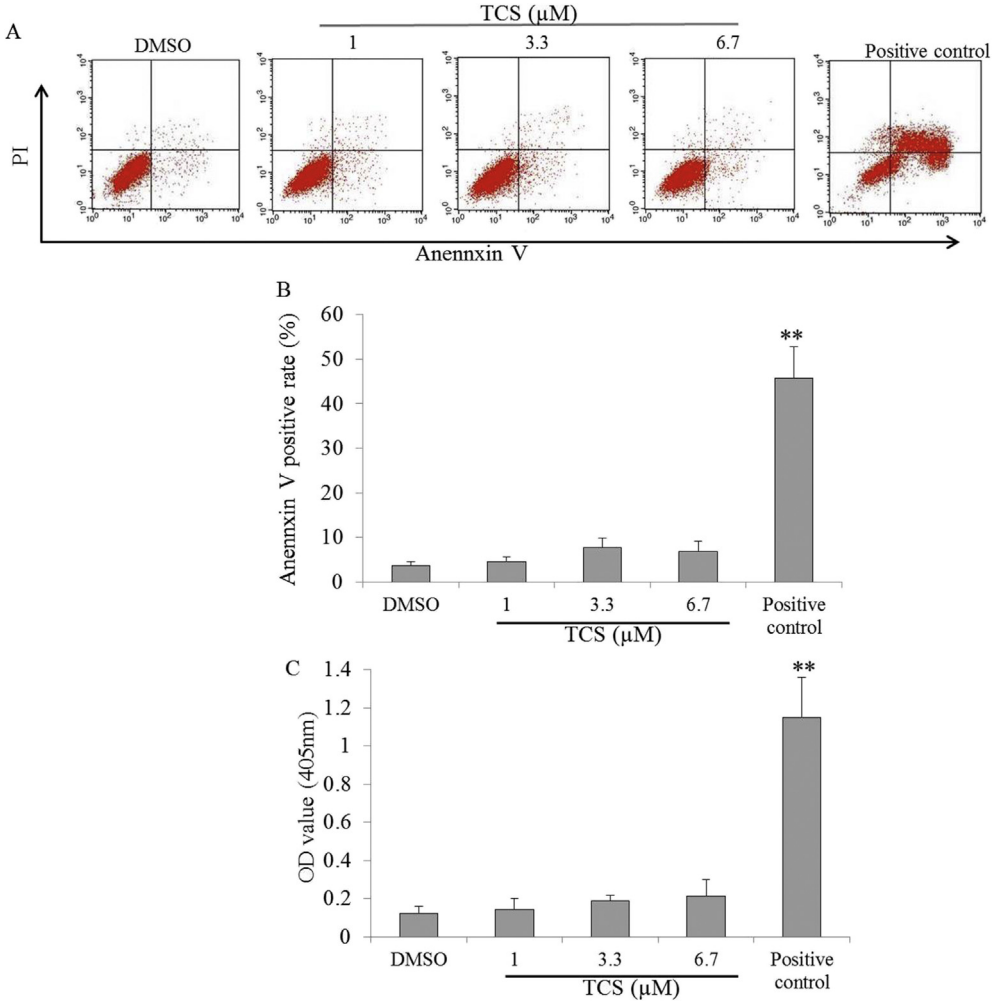

Fig. 2. Treatment with TCS did not induce apoptosis of MKN-45 cells. (A) The cells (1×10^5) were incubated with different dosage of TCS for 24 h. Flow cytometric analysis of apoptotic cell ratios after Annexin V-FITC/PI staining (SubG1 cells). The data are presented as the mean ± SD, n = 3. (B) Quantification of flow cytometric analysis. The data are presented as the mean ± SD, n = 3. (C) Inactivation of caspase-3 in MKN-45 cells induced by TCS. The cells (1×10^5) were incubated with different dosage of TCS for 24 h. Caspase-3 activities were assayed as described in the materials and methods section. Results are means ± SD, n = 3. $^{**}p < 0.01$ compared with DMSO group.

values are presented as mean ± SD Significance was set at $p < 0.05$ for all tests.

3. Results

3.1. TCS significantly inhibited the growth of MKN-45 cells in a time and dose dependent manner, which was independent of apoptosis

To detect the anti-tumor effects of TCS on MKN-45 cells, the cells were cultured with 0–10 μM TCS for 24, 48 and 72 h. The results demonstrated that TCS inhibited MKN-45 cell growth in a time and dose-dependent manner (Fig. 1A). The morphologic changes also confirmed the inhibition of TCS on MKN-45 cells (Fig. 1B). Cytoplasmic shrinkage, membrane blebbing and nuclear condensation were observed.

Then we examined if TCS could induce apoptosis in MKN-45 cells by using the Annexin V-FITC/PI Apoptosis Detection Kit. We found that MKN-45 cells treated with different concentrations of TCS for 48 h without engendering the early apoptotic cells comparing with the positive control (Fig. 2A,B). Meanwhile, the effect of TCS on apoptosis MKN-45 cells was also tested by measuring caspase-3 activity. We observed that there is no difference between control and TCS-treated groups. Together, the results above suggested that TCS inhibited MKN-45 cells growth was independent from apoptosis.

3.2. TCS dose-dependently induced autophagy in MKN-45 cells

To investigate the death of TCS in MKN-45 cells, the monodansylcadaverine (MDC) staining analysis were implemented, which was able to specifically stain autophagosomes. The results indicated that TCS caused a significantly increase in the number of MDC-labeled autophagolysosomes in the cells compared with the control group. Flow cytometric analysis also showed that the MDC-positive cells caused by treatment with TCS were increased in a dose-dependent manner (Fig. 3A,B). Autophagy is characterized by activation of Atg-5 and LC3. Endogenous LC3 I proteins conjugated with PE to form LC3 II under stress or infection conditions (25). On the contrary to the cytoplasmic localization of LC3I, LC3 II bonded with both the outer and inner membranes of autophagosome, therefore being a typical marker of autophagy formation (26). Atg5, an essential protein for autophagosome formation, is also an useful marker protein (27). Western blot analysis revealed that the upregulation of Atg5 and the conversion from LC3 I to LC3 II were detected in TCS treated cells in a dose-dependent manner (Fig. 3C). These results demonstrated that TCS induced autophagy in MKN-45 cells.

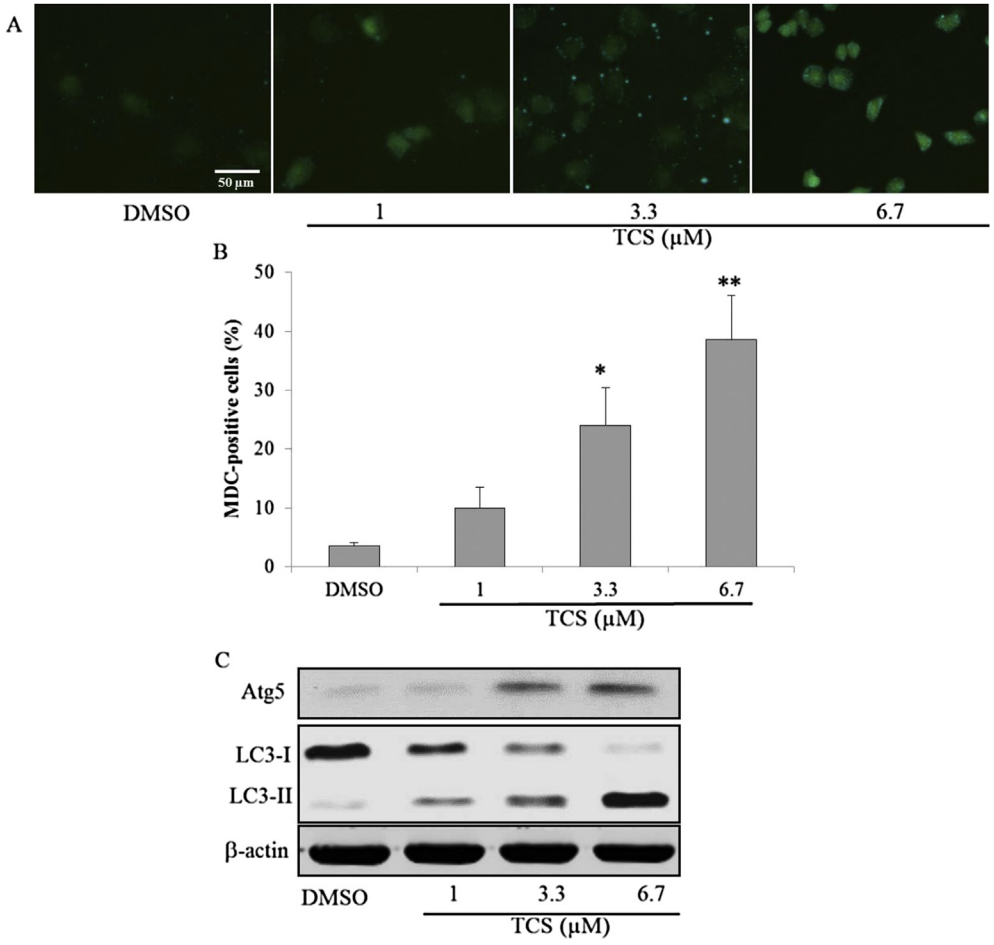

Fig. 3. TCS induced MKN-45 cells autophagy. (A) The cells (1×10^5) were incubated with different concentration of TCS for 24 h. Changes of fluoresce intensity were observed by fluorescence microscopy with MDC staining (200× magnification). (B) The MDC positive ratio was detected by flow cytometric analysis. Results are expressed as mean value ± SD for five independent experiments. $^{**}p < 0.01$ and $^{*}p < 0.05$ compared with TCS–untreated group. (C) MKN-45 were lysed after the treatment with different concentration of TCS for 24 h, and the protein levels of LC3 and Atg5 were detected by western blot analysis, n = 3.

3.3. TCS induced autophagy was dependent on ROS generation

To determine the function of ROS in TCS induced autophagy in MKN-45 cells, the intracellular ROS level was measured by flow cytometric analysis stained with DCF-DA. Our results indicated that TCS treatment induced intracellular ROS generation in a dose-dependent manner. The growth of ROS generation almost inhibited by pretreated with NAC (Fig. 4A). The MDC positive ratio decreased notably in NAC treated MKN-45 cells (Fig. 4B). To investigate the interaction of autophagy and ROS in TCS-treated MKN-45 cells, 3-MA, a specific autophagy inhibitor, as well as NAC and ROS scavenger were employed. The results proved that TCS-induced ROS generation was stable by 3-MA treated, but TCS induced cell autophagy partially reversed by pretreatment with NAC (Fig. 4B). Taken together, these results indicated that the generation of ROS induced by TCS intensified autophagic process in MKN-45 cells.

3.4. TCS induced autophagy via up-regulation of NF-κB and p53 pathways in MKN-45 cells

Western blot analysis was carried out to test the underlying mechanisms of TCS-induced autophagy. The results showed treatment with TCS resulted in the level of p-NF-κB and p-p53 up-regulation. Moreover, in order to clarify the sequence of ROS and NF-κB/p53 on TCS induced cell death, the ROS scavenger NAC was used. Comparing with TCS alone treatment, the level of p-NF-κB and p-p53 were decreased by the pretreatment with NAC. While the cells were exposure to autophagy inhibitor 3 MA, the level of those proteins was unchanged (Fig. 4C). Moreover, NF-κB or p53 inhibitor could partially reverse TCS-induced autophagy in the cells (Fig. 4D,E). Above all, the results indicated that TCS-treatment in MKN-45 cells, first induced the generation of ROS, and then regulated those protein levels and finally inducing autophagy (Fig. 4F).

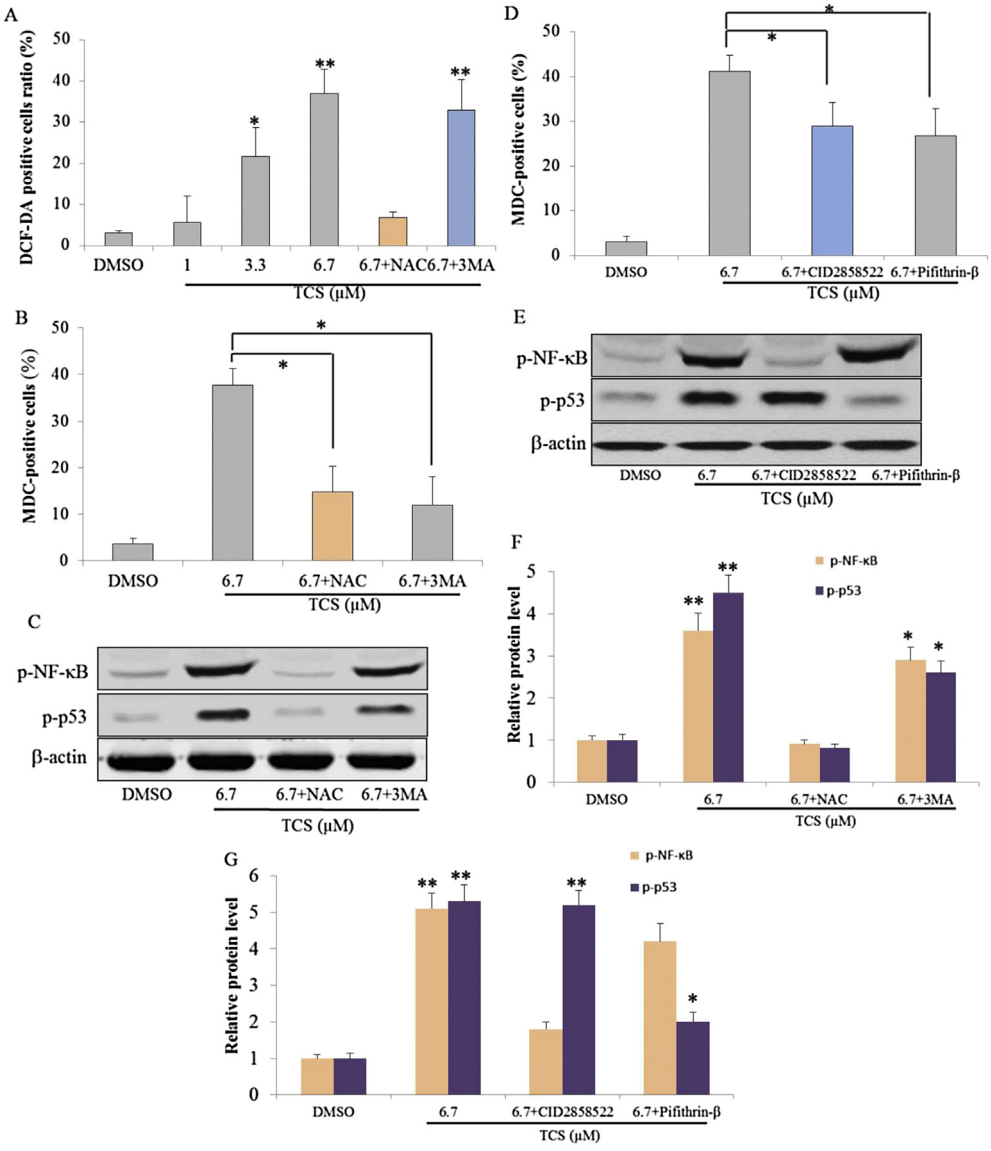

Fig. 4. TCS induced autophagy via a reactive oxygen species (ROS)-dependent way. (A) The DCF-DA positive ratio was detected by flow cytometric analysis in the presence or absence of TCS, NAC, and 3 MA. (B) The MDC positive ratio was detected by flow cytometric analysis in the presence or absence of TCS, NAC, and 3 MA (C) MKN-45 cells were incubated with 6 μM TCS in the presence or absence of NAC (4 μM) or 3 MA (5 μM) for 24 h, and then the protein levels of p-NF-κB, and p-p53 were detected by western blot analysis. (D, E) The MDC positive ratio was detected by flow cytometric analysis in the presence or absence of TCS, CID2858522, and Pifithrin-β, and then the protein levels of p-NF-κB, and p-p53 were detected by western blot analysis. (F, G) Quantification analysis of proteins expression level (normalized to β-actin). Results are expressed as mean value ± SD, n = 3. $^{**}p < 0.01$ and $^{*}p < 0.05$ compared with TCS−untreated group.

3.5. TCS inhibited MKN-45 xenografts tumor growth and regulated the expression of autophagy related proteins

To investigate the effect of TCS on tumor growth *in vivo*, we developed an animal model of MKN-45, and the tumor formation was also monitored. In the end of study, the expression of associated proteins was measured by western blotting assay. After treatment with TCS for 3 weeks, the tumors in each group were harvested and weighted. As a result, the TCS inhibited MKN-45 xenografts tumor growth in a dose-dependent manner (Fig. 5A,B). The expression of Atg5 and the conversion from LC3 I to LC3 II in xenografts was significantly upregulated after treatment with TCS (Fig. 5C,D). The results of TCS used in mouse model were consistent with *in vitro* study.

4. Discussion

Gastric cancer with more than 70% occurring rate in developing countries in 2013 was ranked as the second leading cause of cancer mortality of the same year, making it one of the common malignancies (28). At present, the conventional treatment strategy for gastric cancer is surgery. However, some patients diagnosed with gastric cancer in later stages, are not eligible for surgeries. For patients with advanced gastric cancer, chemotherapy is the common treatment strategy instead of surgery. But in recent years, the growing concerns of chemotherapy side effects makes the gastric cancer patients call for a new gastric cancer treatment strategy.

As reported previously, TCS is able to induce apoptosis in many cell lines. In this study, we implemented the Annexin V-FITC/PI Apoptosis Detection Kit and caspase-3 activity in order to test whether TCS induced MKN-45 cells apoptosis. The experiments results indicated that TCS could not induce MKN-45 cells apoptosis. Then we carried out several additional studies, such as conversion of LC3 I to LC3 II, the expression of ATG5, flow cytometric analysis and morphology to demonstrate TCS could induce autophagy in the MKN-45 cells. To our knowledge, this is the first time to propose that TCS-induced autophagy in human gastric cancer cells.

In stomach adenocarcinoma, TCS induced apoptosis through p53-p21 pathway. We suspected that if p53 was involved in the occurrence of autophagy or not. Therefore we detected the expression of p53. The results showed that TCS upregulated the expression of p-p53, indicating that p53 was a mediator in TCS-induced autophagy. NF-κB, a major regulator of cell survival, is closely involved in carcinogenesis. The requirement of NF-κB activation in autophagy has already been proved in previous studies (10). In this study, our results the level of p-NF-κB increased after treatment with TCS. This finding indicated that NF-κB also acted as a mediator of TCS-induced autophagy. NF-κB worked together with other important oncogenic signaling pathways, including Ras, p53 and notch signaling (29). Nevertheless, the stability of p53 is regulated by E3 ubiquitin ligase MDM2 through inducing proteasome-dependent degradation of p53. NF-κB induces MDM2 transcription, thereby decreasing p53 abundance and contributing to the survival and tumor-promoting abilities of NF-κB (29). It was also demonstrated that p53 and NF-κB could cooperate in the activation of autophagy (30). Further studies are needed to investigate the interaction between p53 and NF-κB in TCS-induced autophagy in MKN-45 cells.

ROS acts as a possible mediators of cellular injury through non-specific modification and disruption of proteins, phospholipids and nucleic acids (31). ROS has been implicated in both the induction of apoptosis and autophagy (7, 32–34). Zhang C et al reported that

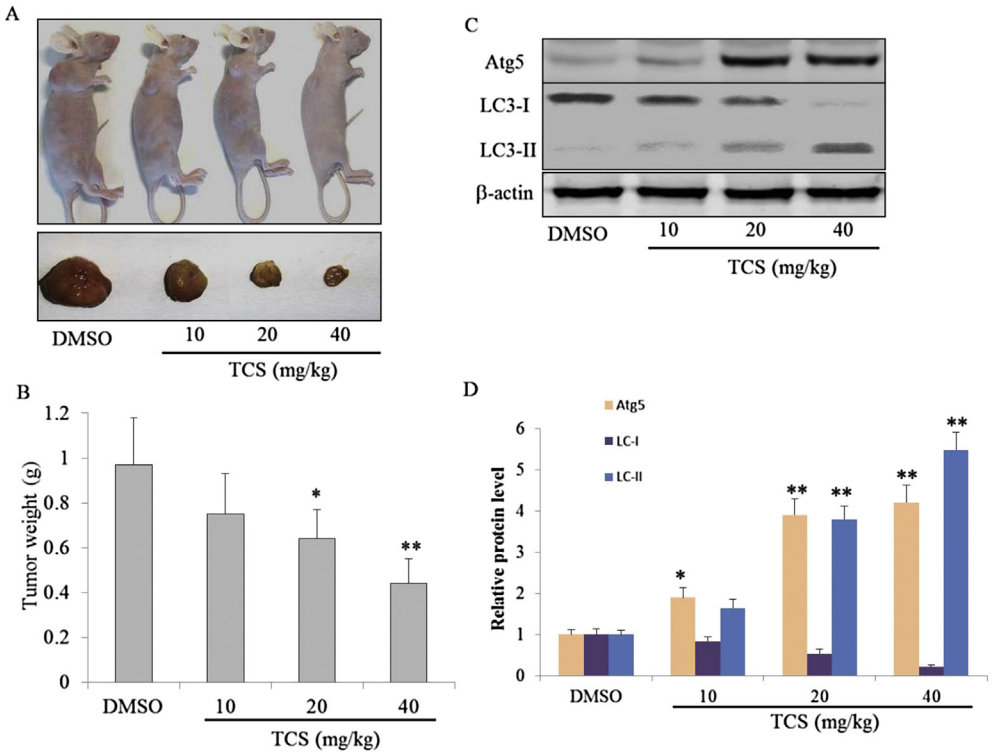

Fig. 5. TCS inhibits MKN-45 xenograft growth in nude mice via inducing autophagy. (A) Twenty-four BALB/c nude mice received a subcutaneous injection of MKN-45. After the tumor growth, the mice were divided into 4 groups and orally administered of vehicle, 10, 20 or 40 mg/kg TCS once daily for three weeks. In the end of study, the mice were sacrificed and excised tumors were shown. (B) The tumor weight in each groups were weighted by balance. (C) The expressions of LC3 and Atg5 in tumor tissues were analyzed by Western blotting. (D) Quantification analysis of proteins expression levels (normalized to β-actin). Results are expressed as mean value ± SD, n = 8. $^{**}p < 0.01$ and $^{*}p < 0.05$ compared with TCS–untreated group.

ROS involved in TCS-induced apoptosis of human choriocarcinoma cells (35). Similarly, the generation of ROS was also detected in TCS-induced autophagy in MKN-45 cells, indicating that the ROS play a role in autophagy. In addition, pretreatment with NAC almost inhibited TCS-induced autophagy, while pretreatment with 3-MA, the generation of ROS did not change, showing that TCS-induced autophagy might be modulated via the generation of ROS.

A number of studies disclosed the relationship between ROS generation and levels of autophagy related proteins including NF-kB and p53. It is known that oxidative stress is an upstream event to influence both NF-κB and p53-based signaling responses (36). Therefore ROS is also a secondary messenger to activate many host signaling responses, including NF-kB and p53 (37). These previous studies lead to a question of whether increased ROS play a role in TCS-induced autophagy. To test this possibility, NAC pretreatment decrease the level of p- NF-kB and p-p53, indicating that the generation of ROS regulating the expression of NF-kB and p53 pathway. The presence of 3-MA or not made no difference to the level of those protein compared with TCS-treated. As a result, the generation of ROS trigged the activation of p53 and NF-kB before inducing autophagy.

By establishing the MKN-45 xenograft model, we also assessed the anti-tumor effect of TCS in MKN-45 *in vivo*. We found that TCS inhibited the growth of MKN-45. The tumors of the vehicle group had more aggressive phenotype and were more prominent compared with the TCS-treated groups. Moreover, the protein expressions of Atg-5, LC3 II in tumor tissues were upregulated by TCS. All these *in vivo* results were certainly consistent with the results *in vitro*.

In conclusion, our study unveils a novel mechanism of drug action that TCS induced autophagy in MKN-45 cells, accompanied by up-regulation of NF-kB and p53, via the generation of ROS. The results indicate that TCS may be a potential candidate as an active agent for treating gastric cancer.

Conflict of interest

The authors declare that they have no competing interests.

References

(1) Chen S, Rehman SK, Zhang W, Wen A, Yao L, Zhang J. Autophagy is a therapeutic target in anticancer drug resistance. Biochim Biophys Acta. 2010;1806:220–229.
(2) Denton D, Xu T, Kumar S. Autophagy as a pro-death pathway. Immunol Cell Biol. 2015;93:35–42.
(3) Kabeya Y, Mizushima N, Ueno T, Yamamoto A, Kirisako T, Noda T, et al. LC3, a mammalian homologue of yeast Apg8p, is localized in autophagosome membranes after processing. EMBO J. 2000;19:5720–5728.
(4) Nathan C. Specificity of a third kind: reactive oxygen and nitrogen intermediates in cell signaling. J Clin Invest. 2003;111:769–778.
(5) Narayanan A, Amaya M, Voss K, Chung M, Benedict A, Sampey G, et al. Reactive oxygen species activate NFkappaB (p65) and p53 and induce apoptosis in RVFV infected liver cells. Virology. 2014;449:270–286.
(6) M1 Qi, Fan S, Yao G, Li Z, Zhou H, Tashiro S, et al. Pseudolaric acid B-induced autophagy contributes to senescence via enhancement of ROS generation and mitochondrial dysfunction in murine fibrosarcoma L929 cells. J Pharmacol Sci. 2013;121:200–211.
(7) Azad MB, Chen Y, Gibson SB. Regulation of autophagy by reactive oxygen species (ROS): implications for cancer progression and treatment. Antioxid Redox Signal. 2009;11:777–790.
(8) Morgan MJ, Liu ZG. Crosstalk of reactive oxygen species and NF-kappaB signaling. Cell Res. 2011;21:103–115.
(9) Chang CP, Su YC, Lee PH, Lei HY. Targeting NFKB by autophagy to polarize hepatoma-associated macrophage differentiation. Autophagy. 2013;9:619–621.
(10) Criollo A, Chereau F, Malik SA, Niso-Santano M, Marino G, Galluzzi L, et al. Autophagy is required for the activation of NFkappaB. Cell Cycle. 2012;11:194–199.
(11) He H, Zang LH, Feng YS, Chen LX, Kang N, Tashiro S, et al. Physalin A induces apoptosis via p53-Noxa-mediated ROS generation, and autophagy plays a protective role against apoptosis through p38-NF-kappaB survival pathway in A375-S2 cells. J Ethnopharmacol. 2013;148:544–555.
(12) Karin M. Nuclear factor-kappaB in cancer development and progression. Nature. 2006;441:431–436.
(13) Krejci O, Wunderlich M, Geiger H, Chou FS, Schleimer D, Jansen M, et al. p53 signaling in response to increased DNA damage sensitizes AML1-ETO cells to stress-induced death. Blood. 2008;111:2190–2199.
(14) Yamaguchi T, Miki Y, Yoshida K. Protein kinase C delta activates IkappaB-kinase alpha to induce the p53 tumor suppressor in response to oxidative stress. Cell Signal. 2007;19:2088–2097.
(15) Sha O, Niu J, Ng TB, Cho EY, Fu X, Jiang W. Anti-tumor action of trichosanthin, a type 1 ribosome-inactivating protein, employed in traditional Chinese medicine: a mini review. Cancer Chemother Pharmacol. 2013;71:1387–1393.
(16) Au TK, Collins RA, Lam TL, Ng TB, Fong WP, Wan DC. The plant ribosome inactivating proteins luffin and saporin are potent inhibitors of HIV-1 integrase. FEBS Lett. 2000;471:169–172.
(17) Byers VS, Levin AS, Malvino A, Waites L, Robins RA, Baldwin RW. A phase II study of effect of addition of trichosanthin to zidovudine in patients with HIV disease and failing antiretroviral agents. AIDS Res Hum Retrovir. 1994;10:413–420.
(18) Sha O, Yew DT, Ng TB, Yuan L, Kwong WH. Different in vitro toxicities of structurally similar type I ribosome-inactivating proteins (RIPs). Toxicol Vitro. 2010;24:1176–1182.
(19) Ng TB, Wong JH, Wang H. Recent progress in research on ribosome inactivating proteins. Curr Protein Pept Sci. 2010;11:37–53.
(20) Zhu Y, Sun Y, Cai Y, Sha O, Jiang W. Trichosanthin reduces the viability of SUDHL2 cells via the activation of the extrinsic and intrinsic apoptotic pathways. Mol Med Rep. 2015;13:403–411.
(21) Fang EF, Zhang CZ, Zhang L, Wong JH, Chan YS, Pan WL, et al. Trichosanthin inhibits breast cancer cell proliferation in both cell lines and nude mice by promotion of apoptosis. PLoS One. 2012;7:e41592.
(22) Kang M, Ou H, Wang R, Liu W, Mao Y, Tang A. Effect of trichosanthin on apoptosis and telomerase activity of nasopharyngeal carcinomas in nude mice. J BUON. 2013;18:675–682.
(23) Zhang D, Lu LM, Chen B, Li Q, Zhou J, Tao L. Thrichosanthin enhances cisplatin-induced laryngocarcinoma apoptosis through inhibiting transcription factor nuclear factor kappaB. Zhonghua Er Bi Yan Hou Tou Jing Wai Ke Za Zhi. 2013;48:322–328.
(24) Xu J, Gao DF, Yan GL, Fan JM. Induced apoptotic action of recombinant trichosanthin in human stomach adenocarcinoma MCG803 cells. Mol Biol Rep. 2009;36:1559–1564.
(25) Ichimura Y, Imamura Y, Emoto K, Umeda M, Noda T, Ohsumi Y. In vivo and in vitro reconstitution of Atg8 conjugation essential for autophagy. J Biol Chem. 2004;279:40584–40592.
(26) Li P, Shi J, He Q, Hu Q, Wang YY, Zhang LJ, et al. *Streptococcus pneumoniae* induces autophagy through the inhibition of the PI3K-I/Akt/mTOR pathway and ROS hypergeneration in A549 cells. PLoS One. 2015;10:e0122753.
(27) Mizushima N, Ohsumi Y, Yoshimori T. Autophagosome formation in mammalian cells. Cell Struct Funct. 2002;27:421–429.
(28) Fitzmaurice C, Dicker D, Pain A, Hamavid H, Moradi-Lakeh M, MacIntyre MF, et al. The global burden of cancer 2013. JAMA Oncol. 2015;1:505–527.
(29) Oeckinghaus A, Hayden MS, Ghosh S. Crosstalk in NF-kappaB signaling pathways. Nat Immunol. 2011;12:695–708.
(30) Shen W, Chen D, Liu S, Chen L, Yu A, Fu H, et al. S100A4 interacts with mutant p53 and affects gastric cancer MKN1 cell autophagy and differentiation. Int J Oncol. 2015;47:2123–2130.
(31) Chtourou Y, Aouey B, Kebieche M, Fetoui H. Protective role of naringin against cisplatin induced oxidative stress, inflammatory response and apoptosis in rat striatum via suppressing ROS-mediated NF-kappaB and P53 signaling pathways. Chem Biol Interact. 2015;239:76–86.
(32) Scherz-Shouval R, Elazar Z. ROS, mitochondria and the regulation of autophagy. Trends Cell Biol. 2007;17:422–427.
(33) Johansson I, Monsen VT, Pettersen K, Mildenberger J, Misund K, Kaarniranta K, et al. The marine n-3 PUFA DHA evokes cytoprotection against oxidative stress and protein misfolding by inducing autophagy and NFE2L2 in human retinal pigment epithelial cells. Autophagy. 2015;11:1636–1651.
(34) Fiers W, Beyaert R, Declercq W, Vandenabeele P. More than one way to die: apoptosis, necrosis and reactive oxygen damage. Oncogene. 1999;18:7719–7730.
(35) Zhang C, Gong Y, Ma H, An C, Chen D, Chen ZL. Reactive oxygen species involved in trichosanthin-induced apoptosis of human choriocarcinoma cells. Biochem J. 2001;355:653–661.
(36) Pallichankandy S, Rahman A, Thayyullathil F, Galadari S. ROS-dependent activation of autophagy is a critical mechanism for the induction of anti-glioma effect of sanguinarine. Free Radic Biol Med. 2015;89:708–720.
(37) Gwinn MR, Vallyathan V. Respiratory burst: role in signal transduction in alveolar macrophages. J Toxicol Environ Health B Crit Rev. 2006;9:27–39.